

New approach for design and development of multi-role aerial module for management of the pedological drought

DOI: 10.35530/IT.076.04.2022150

MIHAELA JOMIR
BOGDAN CAZAN
MARIAN-CATALIN GROSU
ADRIAN SALISTEAN

ALINA-FLORENTINA VLADU
OVIDIU IORDACHE
RAZVAN-VICTOR SCARLAT

ABSTRACT – REZUMAT

New approach for design and development of multi-role aerial module for management of the pedological drought

Soil drought, seen as the depletion of soil water reserves at watering depths below the readily accessible water content, is a challenging problem for humanity, with a massive negative impact on social, economic, and environmental activities. This paper proposes a new approach to the management of soil-induced drought disasters.

In this respect, 8 variants of fabrics (used as matrices of composite materials) and 3 variants of composite structures, used in the construction of collapsible multi-roll aerial modules for soil drought, have been developed and tested in INCDTP-accredited laboratories. Thus, the structures have been tested in terms of tensile behaviour, the strength and elongation at break, respectively the strength and elongation at tear. The experiments carried out, as well as the experience of specialists in the design of technical textile structures for special applications, have shown that the manufacturing of textile supports used as matrices for composite materials used in the construction of collapsible multi-roll aerial modules for pedological drought, structures specific to textile articles with special uses are used, for which programming schemes have been obtained.

The particularly restrictive conditions imposed by the field of use, in conjunction with the values obtained from the physical-mechanical testing of composite fabrics and structures, required the use of specialised software to obtain digital solutions. The results obtained as a result of FEM simulation predicted the behaviour of textile structures, composites, and the air module under dynamic conditions.

Keywords: multi-roll aerial module, pedological drought, aerial mulching, CAD-CAM, modelling, FEM

O nouă abordare pentru proiectarea și dezvoltarea unui modul aerian multirol pentru gestionarea secetei pedologice

Seceta pedologică, văzută ca epuizarea rezervei de apă din sol la adâncimi de udare sub conținutul de apă ușor accesibil, este o problemă provocatoare pentru umanitate, cu un impact negativ masiv asupra activităților sociale, economice și asupra mediului.

Această lucrare propune o nouă abordare a managementului calamităților declanșate de seceta pedologică.

În acest sens, au fost dezvoltate și testate în laboratoarele acreditate ale INCDTP 8 variante de țesături (utilizate ca matrici ale materialelor compozite) și 3 variante de structuri compozite, utilizate la construcția modulelor aeriene colapsabile multirol pentru seceta pedologică. Astfel, structurile au fost testate din punct de vedere al comportării la tracțiune, fiind determinate forța și alungirea la rupere, respectiv forța și alungirea la sfârșiere. Experimentările realizate, precum și experiența specialiștilor în proiectarea structurilor textile tehnice pentru aplicații speciale au evidențiat faptul că, pentru realizarea suporturilor textile utilizate ca matrici pentru materialele compozite utilizate la construcția modulelor aeriene colapsabile multirol pentru seceta pedologica se utilizează structuri specifice articolelor textile cu utilizări speciale, pentru care au fost obținute schemele de programare.

Condițiile deosebit de restrictive impuse de domeniul de utilizare, coroborate cu valorile obținute în urma testării fizico-mecanice a țesăturilor și structurilor compozite, au impus utilizarea unui software specializat pentru obținerea soluțiilor digitale. Rezultatele obținute ca urmare a simulării cu FEM au predicționat comportarea în condiții dinamice a structurilor textile, materialelor compozite și implicit a modulului aerian.

Cuvinte-cheie: modul aerian multirol, secetă pedologică, mulcire aeriană, CAD-CAM, modelare, FEM

INTRODUCTION

Extreme weather events in recent years have shown that the Earth's health is deteriorating at an accelerating rate. Dry areas on the Earth's surface have increased and are susceptible to accelerated degradation and desertification through loss of fertility

[1–3]. Desertification is a real threat, provoked both by human activities (excessive or inefficient water use, overgrazing and deforestation, excessive urbanisation and industrialisation, etc.) and climate change (rising average temperatures, increasing intensity and frequency of droughts and other extreme weather events, etc.) [2–5].

Soil is the “fragile skin” that anchors all life on Earth and from which biodiversity springs, and it has been damaged by almost 50% in the last 150 years of its existence [3, 6].

According to the European Commission’s World Atlas of Desertification, more than 75% of the land is already degraded, and more than 90% could be degraded by 2050. Globally, a total area the size of the EU (~ 4 million km²) is being degraded every year, with economic impacts of billions of euros annually. At the same time, the accelerating loss of forests will make mitigation efforts more challenging [4, 7, 8]. Global warming exacerbates droughts and concurrent heat waves in many parts of the world, leading to an increase in the frequency of natural disasters such as severe vegetation fires, and significant impacts on water resources and human health [6, 9]. The depletion of the soil water reserve at watering depths below the readily accessible water content is considered a “pedological drought”. In terms of agrometeorological drought indices, the moisture level generates 3 levels of pedological drought: moderate (35% – 50%), severe (20%–35%), and extreme – below the wilting point (0%–20%) [10, 11]. When lands are extremely dry, they are susceptible to erosion, and the topsoil is rapidly removed, further degrading the land surface. When talking about forested areas, fires and irresponsible logging are major causes of soil erosion [12, 13]. Measures to mitigate post-fire erosion mainly aim at reducing the kinetic energy of raindrops that would cause heavy run-off, thus enhancing water infiltration and limiting the detachment and transport of soil particles [8, 14]. This is achieved either by creating physical barriers on slopes and in the catchment, by building gabion-like structures for hydrological routing and control, or by covering the burnt soil with organic or inorganic protective layers (“mulching”) or by vegetation recovery [9]. Mulch layers are most often in the form of agricultural residues

(wheat, barley, or rye straw) or heterogeneous wood residues produced “in situ” or “ex-situ” (chips, shavings, chips of saw, branches, or from logs. Covering the burnt areas with a medium-thick layer of mulch (about 5 cm) accelerates native vegetation recovery by maintaining moisture and protecting it from heat and solar radiation. This gives the seeds in the soil a better chance to germinate and stabilise the burnt areas. Aerial interventions are a viable solution for soil protection through mulching but require adequate logistics for the storage, transport, and spreading of mulch bales. Among the textile structures used in aerial mulching operations are knitted (knotless) cargo nets, woven or combined polyester (PES), polyamide (PA), or polypropylene (PP) strips.

This paper presents an innovative solution in the field of computer-aided design using specialised software for the realisation of a collapsible multi-roller aerial module for mulching. In this respect, textile moulds used for composite materials and composite fabrics used in the construction of a collapsible multi-roll aerial module for mulching were subjected to experiments.

MATERIALS AND METHODS

Materials used

For a digital design of the modelling and simulation of a multi-role structure intended for interventions in areas affected by soil drought, 8 woven textile structures were tested and analysed, from the point of view of physical-mechanical behaviour (table 1):

- Determination of maximum force and elongation at maximum force using the strip method, according to SR EN ISO 13934-1/2013.
- Determination of tear force of wing-shaped test specimens, according to SR EN ISO 13937-3/ 2000.

The images and graphs from these experiments are presented selectively in figures 1–6 and for the coated fabrics in figures 7–10.

Table 1

PHYSICAL-MECHANICAL BEHAVIOUR OF WOVEN TEXTILE STRUCTURES					
Variant	Raw material		Weave	Yarn fineness	
	warp	weft		warp	weft
T1	100% cotton	100% cotton	1/1	200dtex x 2	200dtex x 2
T2	100% PES	100% PES	D2/1	167dtex/36fx1/150Z	167dtex/36fx1/150Z
T3	100% PES	100% PES	ripstop	76dtex/36fx1/800Z	76dtex/36fx1/350Z
T4	100%PA6.6	100%PA6.6	D2/2	660dtex/120fx1	660dtex/120fx1
T5	100%PES	100%p-aramid 100% PES R: 2:1	R2/1	1100dtex/192fx1/80Z	1100dtex/1192fx1 1100dtex/192fx1/80Z
T6	100%p-aramid	100%p-aramid 100% PES	RB1/2	1670dtex/192fx1/80Z	1670dtex/1192fx1 1100dtex/192fx1/80Z
T7	100%PA6.6	100%PA6.6 100% p-aramid R: 2:2	P2/2	880dtex/120fx1	880dtex/120fx1 660dtex/120fx1
T8	100%PA6.6	100%PA6.6	1/1	660dtex/120fx1	660dtex/120fx1

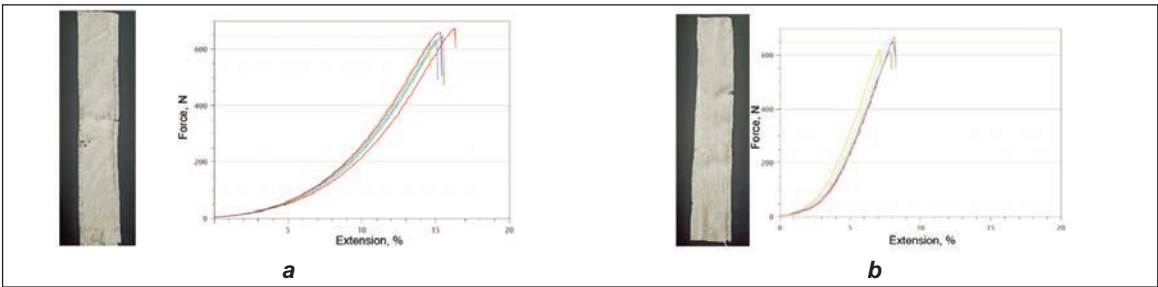


Fig. 1. Maximum breaking force with the strip specimen and corresponding stress-elongation diagrams for 100% cotton fabric (T1): *a* – testing in the warp direction (U); *b* – testing in the weft direction (B)

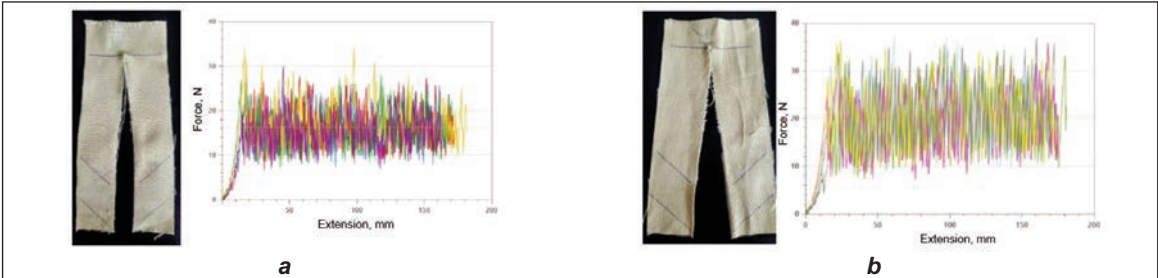


Fig. 2. Maximum tear force with a wing-shaped test piece and the corresponding stress-elongation diagrams for 100% cotton fabric (T1): *a* – testing in the warp direction (U); *b* – testing in the weft direction (B)

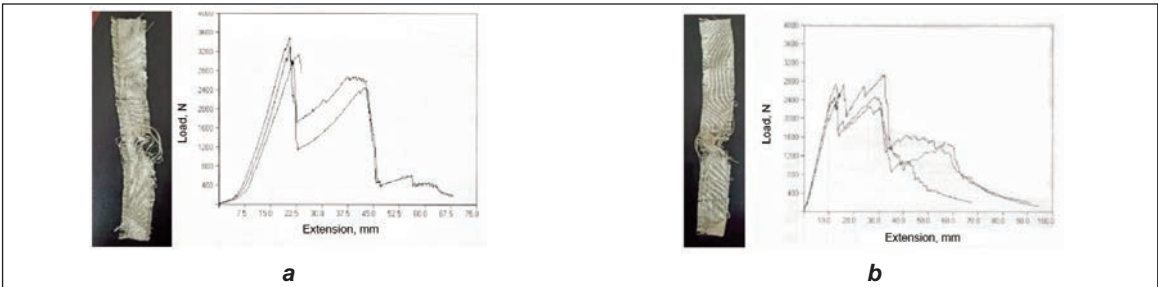


Fig. 3. Maximum breaking force by strip specimen method and corresponding stress-elongation diagrams for fabric 30 % p-aramid / 70 % PES (T5): *a* – testing in the warp direction (U); *b* – testing in the weft direction (B)

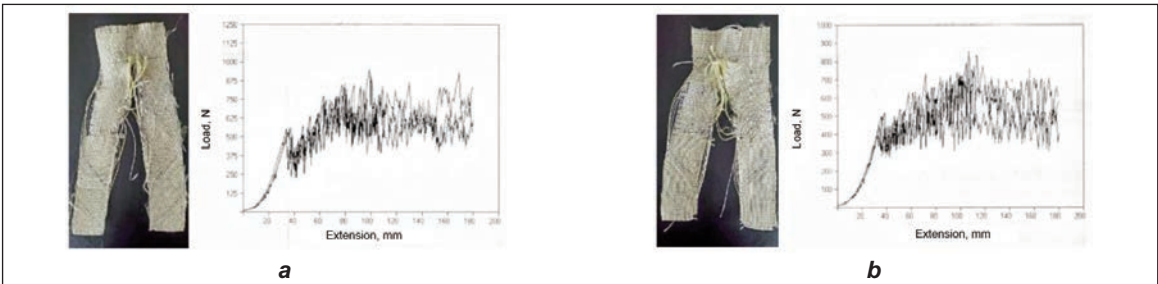


Fig. 4. Maximum tear force of specimens (wing-shaped) and corresponding stress-elongation diagrams for fabric 30 % p-aramid / 70 % PES (T5): *a* – testing in the warp direction (U); *b* – testing in the weft direction (B)



Fig. 5. Maximum breaking force by the strip specimen method and corresponding stress-elongation diagrams for fabric 100% PA 6.6 (T8): *a* – testing in the warp direction (U); *b* – testing in the weft direction (B)

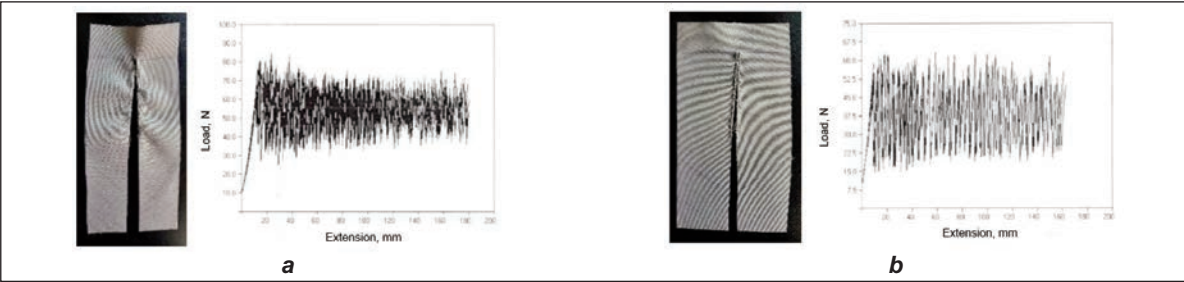


Fig. 6. Maximum tear force of specimens (wing-shaped) and corresponding stress-elongation diagrams for fabric 100% PA 6.6 (T8): *a* – testing in the warp direction (U); *b* – testing in the weft direction (B)

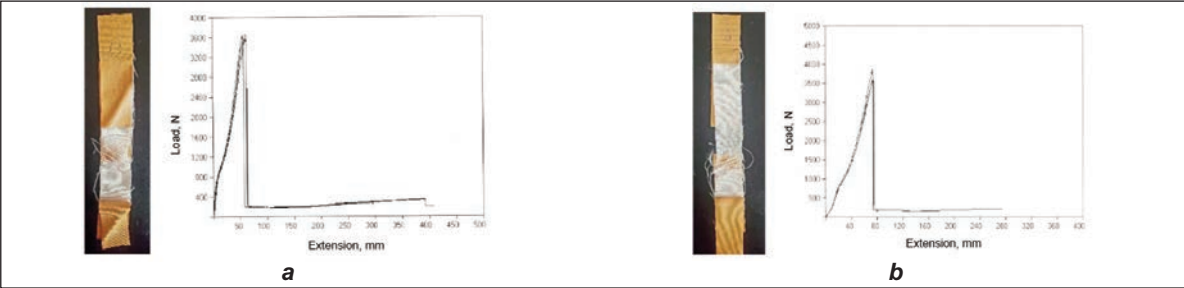


Fig. 7. Maximum breaking force by the strip specimen method and corresponding stress-elongation diagrams for 100% PA6.6 film-coated fabric: *a* – testing in the warp direction (U); *b* – testing in the weft direction (B)

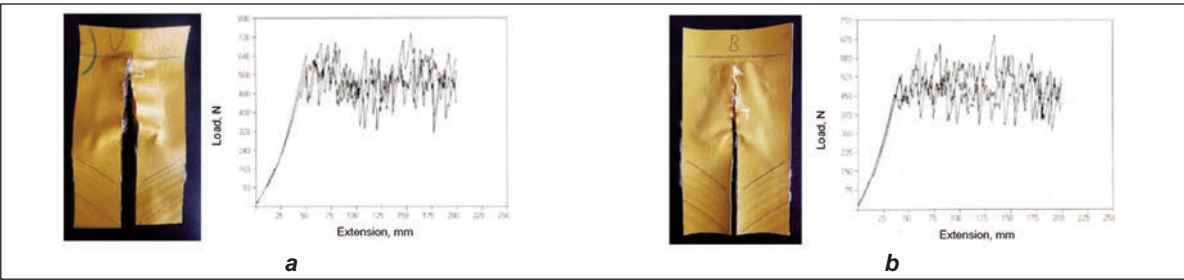


Fig. 8. Maximum tear force of specimens (wing-shaped) and corresponding stress-elongation diagrams for 100% PA6.6 film-coated fabric: *a* – testing in the warp direction (U); *b* – testing in the weft direction (B)



Fig. 9. Maximum breaking force by strip specimen method and corresponding stress-elongation diagrams for fabric 80% p-aramid / 20% PES: *a* – testing in the warp direction (U); *b* – testing in the weft direction (B)



Fig. 10. Maximum tear force of specimens (wing-shaped) and corresponding stress-elongation diagrams for fabric 80% p-aramid / 20% PES: *a* – testing in the warp direction (U); *b* – testing in the weft direction (B)

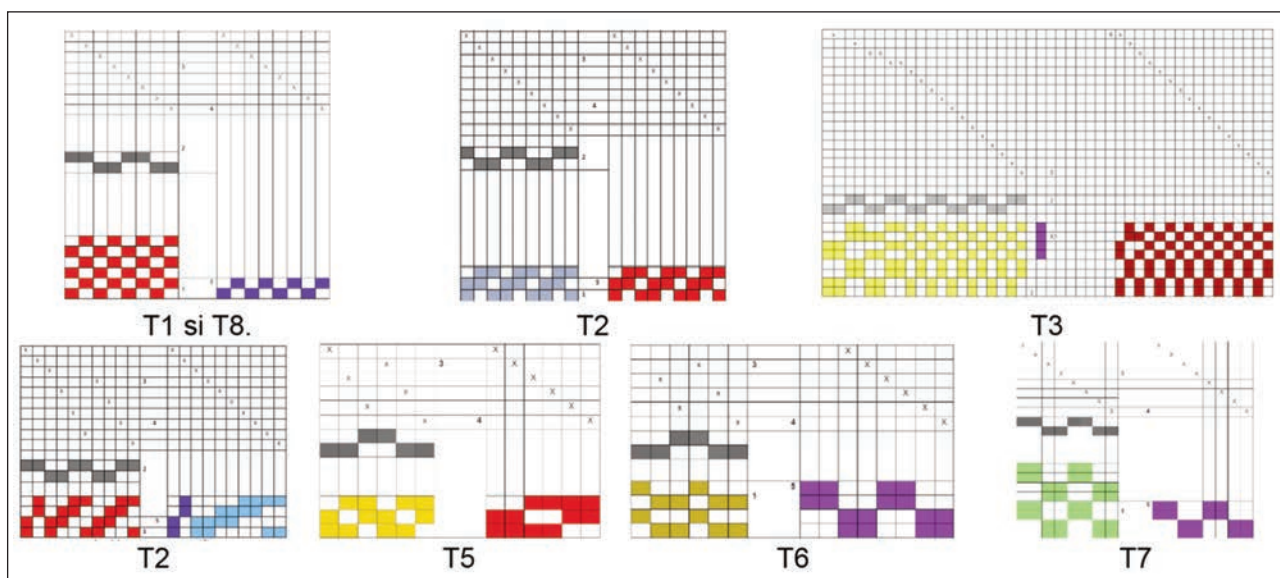


Fig. 11. Programming schemes of woven structures T1 – T8:
1 – weave; 2 – reed; 3 – drawing-in; 4 – sinker command; 5 – pattern card

Programming schemes for textile structures

Experiments carried out in INCDTP-accredited laboratories, as well as the experience of specialists in the design of technical textile structures for special applications have shown that the realization of textile supports used as matrices for composite materials used in the construction of collapsible multi-roller aerial modules for fire and soil drought and of flow arresters, specific structures are used for textile articles with special uses, for which the programming schemes are defined according to figure 11.

CAD for the functional model of a multi-roll collapsible aerial module for soil drought

The digital design carried out by INCDTP specialists, based on the results obtained from the tests and experiments carried out (used as input data), allowed the CAD, with the help of a specialised program, to create the functional model of the collapsible multi-roll aerial module for pedological drought. The CAD model obtained (at $t=0$) for the collapsible aerial module for soil drought is shown in figure 12 (Sketcher and Part Design).

The theoretical foundation of the construction of this type of aerial module was based on the theories of

Fluid Mechanics, which allowed the use of the following working hypotheses:

- a) the environment is continuous for all the situations taken into account, i.e. the mass distribution is considered to be continuous in the occupied volume, from a mathematical point of view, it is considered to be continuous;
- b) the infinitesimal internal forces in the medium are considered to be statistical averages of the interaction forces between the constituent elements, the effect of the static average being independent of the individual state of the constituent elements (solid, in the case of the collapsible multi-roll air module for soil drought);
- c) dA (area) was considered a (sufficiently small) size on which the force dF acts, which does not depend on the individual state of the elements in dA ;
- d) the environment is loaded with concentrated forces F_i and distributed loads p_i , and the external loads give rise to internal forces, hence stresses;
- e) the stress vector (defined as mean values) is defined as $t = \frac{\Delta F}{\Delta A}$ and decomposes into a normal

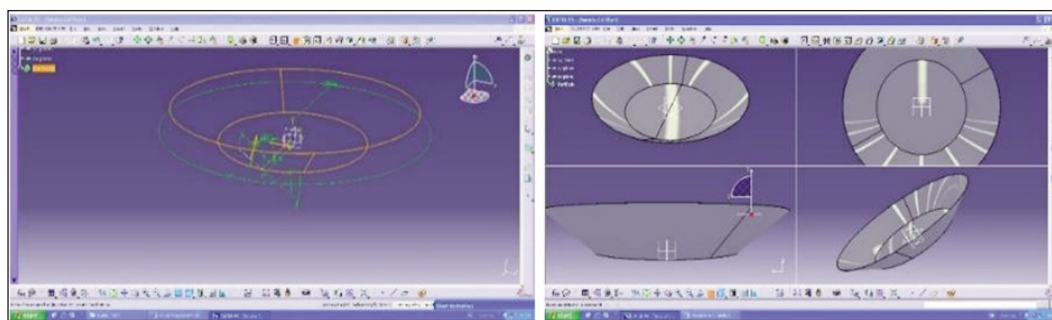


Fig. 12. Digital solution for collapsible aerial mode for soil drought at time $t=0$

component $-\sigma$ and a shear component tangent to the surface τ , these $(\tau_{xy}, \tau_{xz}, \tau_{yx}, \tau_{yz}, \tau_{zx}, \tau_{zy})$ all not being independent;

f) the stress tensor is of the form:

$$\sigma = \begin{bmatrix} \sigma_x & \tau_{xy} & \tau_{xz} \\ \tau_{yx} & \sigma_y & \tau_{yz} \\ \tau_{zx} & \tau_{zy} & \sigma_z \end{bmatrix} = \begin{bmatrix} \sigma_x & \tau_{xy} & \tau_{xz} \\ \tau_{xy} & \sigma_y & \tau_{yz} \\ \tau_{xz} & \tau_{yz} & \sigma_z \end{bmatrix}$$

g) the stress state at a point is defined by equilibrium conditions of the form:

$$\begin{aligned} &\sigma_x dydz - \tau_{yx} dx dz + \left(\sigma_x + \frac{\delta \sigma_x}{\delta x} dx \right) dydz + \\ &+ \left(\tau_{yx} + \frac{\delta \tau_{yx}}{\delta y} dy \right) dx dz + f_x dx dy dz = 0 \\ &\frac{\delta \sigma_x}{\delta x} + \frac{\delta \tau_{yx}}{\delta x} + f_x = 0; \quad \frac{\delta \sigma_y}{\delta y} + \frac{\delta \tau_{xy}}{\delta x} + f_y = 0 \end{aligned}$$

or three-dimensional (for FEM simulation):

$$\begin{aligned} &\frac{\delta \sigma_x}{\delta x} + \frac{\delta \tau_{yx}}{\delta y} + \frac{\delta \tau_{zx}}{\delta z} + f_x = 0; \\ &\frac{\delta \tau_{xy}}{\delta x} + \frac{\delta \sigma_y}{\delta y} + \frac{\delta \tau_{zy}}{\delta z} + f_y = 0; \\ &\frac{\delta \tau_{xz}}{\delta x} + \frac{\delta \tau_{yz}}{\delta y} + \frac{\delta \sigma_z}{\delta z} + f_z = 0; \end{aligned}$$

- h) the variation of stress around an isolated point is demonstrated using a tetrahedron with rectangular surface vectors $\vec{i}, \vec{j}, \vec{k}$ of the axis system;
i) the balance of elementary forces in each direction is:

$$\begin{aligned} \overline{\rho}_x &= \sigma_x \vec{i} + \tau_{xy} \vec{j} + \tau_{xz} \vec{k} \\ \overline{\rho}_y &= \tau_{yx} \vec{i} + \sigma_y \vec{j} + \tau_{yz} \vec{k} \\ \overline{\rho}_z &= \tau_{zx} \vec{i} + \tau_{zy} \vec{j} + \sigma_z \vec{k} \end{aligned}$$

j) the Von Mises criterion (for the interpretation of the Gauss solutions resulting from the simulation) means the probability of occurrence of cracks at the level of the contact of the structure with the fluid) and from a mathematical point of view, represents the square root of the second invariant of the stress tensor, i.e. in Cartesian form:

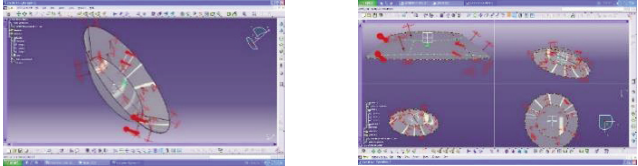
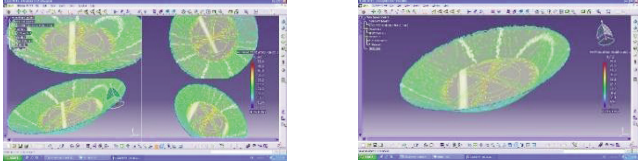
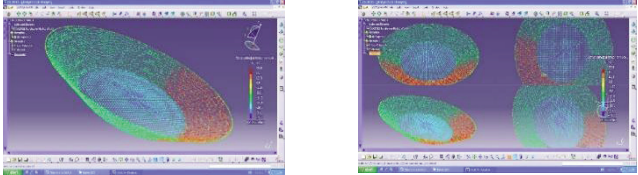
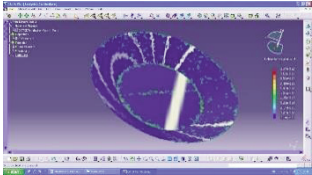
$$J_2 = \tau_{xy}^2 + \tau_{xz}^2 + \tau_{yz}^2 + \frac{1}{6} [(\tau_{yy} - \tau_{zz})^2 + (\tau_{zz} - \tau_{xx})^2 + (\tau_{xx} - \tau_{yy})^2]$$

- k) input for each product considered – represented by: the system of units, the reference system, the geometry of the structure, the material from which the structure is to be made, the type of element for discretising the structure, the type of analysis to be performed, the conditions on the contour (pre-processing stage).
l) the idealisation of the contour was made possible with the help of the sketcher application of the integrated system. The shape of the 2D element that will be the starting point for the 3D model to be subjected to structural analysis, the dimensional constraints, and the 2D and 3D geometries (Part Design) were customised.

RESULTS AND DISCUSSIONS

With the Generative Structural Analysis module, it was possible to generate the finite element structure

Table 2

STRUCTURAL ANALYSIS	
Studied situation	Visuals
View constraints, stresses, and loads	
Von Mises stress (nodal values): [0, 65.2] N_m2	
Stress principal tensor: [-41.8; 25.8] N_m2	
Errors: [2.14e-017; 1.07e-012] J	

in two steps, namely: discretisation and introduction of finite element properties. The FEM model solution created for the MF was done with the help of specialised software. Post-processing allowed visualisation of the results for 3 distinct situations, respectively:

- A. For the situation where the MF has a 5000 kg mass load, $t_0 = 0$ s;
- B. In case MF has deployed a part of the load and has 2000 kg left, $t_1 = t_0 + \varepsilon$ s;
- C. For the situation where MF is empty, $t_2 = t_0 + \varepsilon + \gamma$ s.

The solver included in the program enabled the structural analysis program, which revealed the following: nodal values (Von Mises), principal stress vector, and errors (table 2 for the most difficult situation, i.e. where MF has a 5000 kg mass load, la $t_0 = 0$ s). The stress state (possible cracks) at the contact level of the composite structure with the fluid was predicted using the Von Mises criterion explained above.

CONCLUSIONS

The stress state in the system (possible cracks) likely to occur at the contact of the composite structure with turbulent moving air was predicted using the Von Mises criterion, according to which the solid body boundary state occurs when the shape-modifying specific potential energy reaches the material's characteristic boundary value.

For the composite material from which the collapsible multi-roll module for soil drought is made, a permissible resistance of the order of +009N_m2 is required.

ACKNOWLEDGMENTS

This work was carried out through the Core Programme within the National Research Development and Innovation Plan 2022-2027, carried out with the support of MCID, project no. 6N/2023, PN 23 26, project title "Soluții digitale inovatoare, reziliante, pentru redresarea și creșterea sustenabilă a resurselor naturale terestre și acvatice, precum și pentru valorificarea resurselor energetice aeriene neconvenționale" Acronym: THORR.

REFERENCES

- [1] Bastida, F., Hernández, T., García, C., *Chapter 8 – Soil Erosion and C Losses: Strategies for Building Soil Carbon*, Editor(s): Carlos Garcia, Paolo Nannipieri, Teresa Hernandez, The Future of Soil Carbon, Academic Press, 2018, 215–238, ISBN 9780128116876, <https://doi.org/10.1016/B978-0-12-811687-6.00008-0>
- [2] Niggli, L., Huggel, C., Muccione, V., Neukom, R., Salzmann, N., *Towards improved understanding of cascading and interconnected risks from concurrent weather extremes: Analysis of historical heat and drought extreme events*, Plos Climate, August 10, 2022, <https://doi.org/10.1371/journal.pclm.0000057>
- [3] Andrei, J.V., Avram, S., Băncescu, I., Gâf-Deac, I.I., Gheorghe, C.A., Diaconu, A.I., *Decoupling of CO₂, CH₄, and N₂O agriculture emissions in the EU*, Front. Environ. Sci., Sec. Environmental Economics and Management, Technology-Enabled Circular Economy Practices in Energy Production and Consumption Patterns, 2022, <https://doi.org/10.3389/fenvs.2022.920458>
- [4] World Wildlife Fund, *Soil Erosion and Degradation – Overview*, Available at: <https://www.worldwildlife.org/threats/soil-erosion-and-degradation> [Accessed on August 2022]
- [5] Gâf-Deac Ioan I., et al., *New development: from linear to nonlinear economy. Challenges from the perspective of sustainable development*, W.1, Romania's Sustainable Economic and Social Development. Models, Scenarios, Evaluations, The Romanian Academy, The 3rd Intl. Economic Scientific Research – Theoretical, Empirical and Practical Approaches, ESPERA 2015, ISBN 978-3-631-67330-0, <https://doi.org/10.3726/978-3-653-06571-8>
- [6] Gâf-Deac, I.I., Jaradat, M., Bran, F., Crețu, R.F., Moise, D., Platagea Gombos, S., Breaz, T.O., *Similarities and Proximity Symmetries for Decisions of Complex Valuation of Mining Resources in Anthropically Affected Areas*, In: Sustainability, 2022, 14, 16
- [7] Cherlet, M., Hutchinson, C., Reynolds, J., Hill, J., Sommer, S. and Von Maltitz, G., *World Atlas of Desertification*, Publications Office of the European Union, Luxembourg, 2018, ISBN 978-92-79-75350-3, https://doi.org/10.2760/9205_JRC111155
- [8] Global Drought Risk and Water Stress – DG ECHO Daily Map, 11/10/2019 – World, ReliefWeb, Available at: https://ercportal.jrc.ec.europa.eu/ercmaps/ECMD_20191011_Global_water_stress.pdf [Accessed on August 2022]
- [9] Cook, B.I., Mankin, J.S., Williams, A.P., Marvel, K.D., Smerdon, J.E., Liu, H., 2021: *Uncertainties, limits, and benefits of climate change mitigation for soil moisture drought in Southwestern North America*, In: Earth's Future, 2021, 9, 9, e2021EF002014, <https://doi.org/10.1029/2021EF002014>
- [10] Sandu, I., Mateescu, E., *Monitoring soil drought in Romania and the impact on agriculture*, Inter-Regional Workshop on Indices and Yearly Warning Systems for Drought, Nebraska, USA, 2009
- [11] Panagos, P., Imeson, A., Meusburger, K., Borrelli, P., Poesen, J., Alewell, C., *Soil conservation in Europe: wish or reality?*, In: Land Degrad. Dev., 2016, 27, 1547–1551
- [12] Barkley, Y.C., *After the burn, Assessing and Managing Your Forestland After a Wildfire*, In: Station Bulletin, 2011, 76, May
- [13] Robichaud, P.R., Jordan, P., Lewis, S.A., Ashmun, L.E., Covert, S.A., Brown, R.E., *Evaluating the effectiveness of wood shred and agricultural straw mulches as a treatment to reduce post-wildfire hillslope erosion in southern British Columbia, Canada*, In: Geomorphology, 2013, 197, 21–33, <https://doi.org/10.1016/j.geomorph.2013.04.024>

[14] Barry Cordage Ltd., *Helicopter Cargo Net – 3 000 lb WLL – Model B1*, Available at: <https://www.barry.ca/helicopter-external-load/helicopter-cargo-nets/hcn-b1> [Accessed on August 2022]

Authors:

MIHAELA JOMIR, BOGDAN CAZAN, MARIAN-CATALIN GROSU, ADRIAN SALISTEAN,
ALINA-FLORENTINA VLADU, OVIDIU IORDACHE, RAZVAN-VICTOR SCARLAT

National Research & Development Institute for Textiles and Leather,
16 Lucretiu Patrascanu, 030508, Bucharest, Romania
e-mail: bogdan.cazan@incdtp.ro, adrian.salistean@incdtp.ro, alina.vladu@incdtp.ro,
ovidiu.iordache@incdtp.ro, razvan.scarlat@incdtp.ro

Corresponding author:

MARIAN-CATALIN GROSU
e-mail: catalin.grosu@incdtp.ro